A. VENCL, A. RAC, B. IVKOVIĆ

Investigation of Abrasive Wear Resistance of Ferrous-Based Coatings with Scratch Tester

RESEARCH

Abrasive wear resistance is very important in many applications and in most cases it is directly correlated with hardness of materials. Possible solutions for overcoming poor abrasive wear resistance of light metals, like Al-alloys, is using of coatings. In this paper the investigated results of the two types of ferrous-based coatings were presented and compared with gray cast iron, known as a material with good abrasive wear resistance. Process used for coating deposition on an Al-Si alloy substrate was Atmospheric Plasma Spraying (APS). Scratch tests with diamond indenter were used to simulate abrasive wear process. The indenter velocity of 10 mm/min was used over a wear tracks of 10 mm, with different normal loads applied. Both, coefficient of friction and wear rate of the samples were investigated and analysed in correlation with its mechanical properties.

Keywords: Abrasive wear, ferrous-based coatings, scratch test, atmospheric plasma spraying

1. INTRODUCTION

Abrasion wear is one of the most dominant types of wear, and abrasion wear resistance is very important in many applications. It is well known that hardness of commercially pure metals influence on its abrasive wear resistance and that higher hardness imply a higher wear resistance. Khruschov [1] finds out that increase of the wear resistance depends on the way in which the metal is being hardened (alloying, heat treatment or work-hardening) and that in some cases wear resistance decrease with increase of hardness. The same author establishes a correlation between the abrasive wear resistance and Young's modulus, and showed that wear resistance increase with increase of material Young's modulus [2].

Generally abrasive wear mechanism could be divided in four types: ploughing, cutting, fatigue and fracture (cracking) [3,4], resulting with different surface appearance.

Aluminium alloys have attractive physical and mechanical properties. They are lightweight, low costs production (with sand casting technology), easy to machine and have good recycling possibilities (up to 95 %) [5]. Due to these facts they are often used as a substitution for gray cast iron and steel parts in many industries. Unfortunately tribological properties of Al-alloys are generally poor comparing with gray cast iron or steel. Coatings as a surface engineering treatment are frequently used for improvement of Al-alloys tribological properties.

Since abrasive wear is cumulative actions of the scratches produced by a large number of abrasive particles or hard asperities, a single-point scratch test appears to be a logical way to study the metal removal process. Scratch test offers a possibility for comparison of different materials relatively easy and in short period of time, with good reproducibility. In practice, scratch testing is most often used as a quality control technique enabling the performance of one surface to be qualitatively and, to some extent, quantitatively compared to another which is known to be satisfactory in use [6].

In this paper the investigated results of the two types of ferrous-based coatings were presented and compared with gray cast iron. Process used for coating deposition on an Al-Si alloy substrate was Atmospheric Plasma Spraying (APS).

Aleksandar Vencl, Aleksandar Rac, Faculty of Mechanical Engineering, Tribology Laboratory, Kraljice Marije 16, 11120 Belgrade 35, Serbia, Branko Ivković, Serbian Tribology Society, Sestre Janjić 6, 34000 Kragujevac, Serbia,

2. EXPERIMENTAL DETAILS

2.1. Materials

Substrate material was a Al-Si alloy (EN AlSi10Mg) with following chemical composition: Al-9.8Si-0.48Fe-0.1Cu-0.2Mn-0.3Mg-0.08Zn-0.05Ti (wt. %) and it was produced using sand casting, followed with solution annealing at 540 °C with 35 °C/h, water quenching and artificial ageing at 160±5 °C for 6 h.

Two spray powders were used in this experiment, referred as "A" and "B". The chemical compositions of the powders are shown in Table 1. The powder size was: less than 50 μm and less than 38 μm in diameter for powder "A" and "B", respectively.

A gray cast iron (ref. as SL 26) was chosen as a standard material to compare its performances with the coatings. The chemical composition of this material, fabricated using the sand casting procedure followed with heating at 550 °C in order to eliminate residual stress in the material, is shown in Table 1.

Table 1. Chemical comp. of used powders and SL 26

Powder / material	Element, wt. %						
	C	Si	Mn	P	Cr	Ni	Fe
A	3.5	-	0.35	-	-	-	Balance
B	1.2		1.5		1.3	0.3	Balance
SL 26	3.18	2.17	0.60	0.7	0.37	-	Balance

Coatings deposition was done with Atmospheric Plasma Spraying (APS). Details of the technology process and spray conditions were described elsewhere [7].

2.2. Coatings microstructure

Characterisation of the coatings was done according to the Pratt & Whitney standard [8].

The microstructure of test materials was analysed by optical microscope (OM), where the coatings were sectioned perpendicular to the coated surface. In boat coatings, elongated splats of molten powder form a lamellar structure, with oxide layers in between, typical for spray coatings. No cracking was found in the coatings and no peeling was observed at the interface between the coating and the substrate.

X-ray diffraction (XRD) analysis revealed that A coating structure consists of elemental iron (Fe) and magnetite (Fe_3O_4), while B coating contains elemental iron (Fe) and wustite (FeO). The other phases are present in a small amount, less then 3 %.

Volume fractions of oxides, as well as porosity and unmelted particles, were measured by image analysis software. Oxide content for coating A was approximately 13 % and for coating B was around 41 %. Porosity in the A and B coatings was 2.3 % and 5.8 %, respectively. Volume fraction of unmelted particles in the coating B was approximately 10 %, while unmelted particles were not detected in coating A. It must be mentioned that porosity of the coating B was detected in areas with unmelted particles.

Coating thickness after the machining, tensile bond strength and hardness of tested materials are shown in Table 2.

Table 2. Some physical and mechanical properties

Material	Coating thickness, μm	Tensile bond strength, MPa	Hardness, HV 0.1
A	100	31,08	506
B	170	32,88	433
SL 26	-	-	329

2.3. Abrasion testing

Abrasion wear tests were carried out on the scratch tester "ST - 99" (manufactured by Serbian Tribology Society) under dry conditions, in ambient air at room temperature (≈ 25 °C). A schematic diagram of scratch tester is presented in Figure 1.

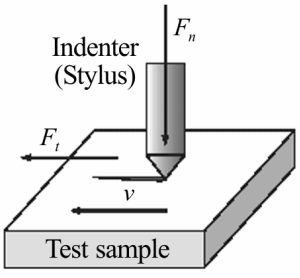

Figure 1. Schematic diagram of scratch tester

Indenter cone was diamond with radius of 0.2 mm. The indenter velocity of 10 mm/min was used over a wear tracks of 10 mm, with different normal loads applied. Two modes of scratch testing were used: PLST (Progressive Loading Scratch Test) and CLST (Constant Load Scratch Test) [9]. In

PLST mode the normal load was increased linearly during the test from 0 to 100 N, while in CLST mode the normal load was constant during the test and was increased step by step between the tests (20, 40, 60, 80 and 100 N).

Before and after testing, both the indenter and the test samples were degreased and cleaned with benzene. Wear scars on test samples were measured on Surface Roughness Measurement System "Talysurf 6", after each test to calculate the volume loss. The values of friction coefficient, normal and friction force were monitored during the test and through data acquisition system stored in the PC.

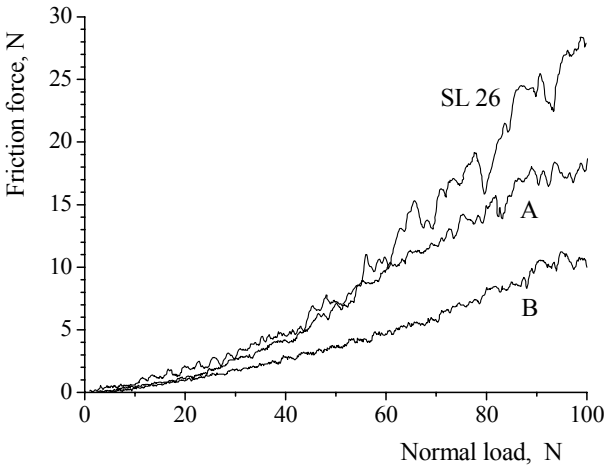

Figure 2. Friction force vs. normal force

3. RESULTS AND DISCUSSION

In order to achieve a higher confidence level in evaluating test results, three replicate tests were run for all tested materials in both, PLST and CLST mode. The results indicate good reproducibility of the wear and friction results.

Dependence of friction force on normal load in PLST mode, for all tested materials, is shown in Figure 2.

Values of friction forces i.e. coefficient of frictions were lowest for coating B followed with coating A and SL 26, with highest values. At lower loads appearance of the curves was straighter than at higher loads where oscillation of friction force occurred with changing of the curve slopes. This indicates the change of wear mechanism and type of deformation under and ahead the indenter.

With the SL 26 change of the curve slope was relatively early, comparing to the coatings. Plastic flow of the material and formation of the micro-chips at the scar edges, typical for ploughing mechanism, was noticed (Fig. 3a). This plastic flow could be the reason why SL 26 shows higher values of coefficient of friction, although it is softer then the both coatings.

With both coatings this plastic flow of the material wasn't noticed in a significant meter. Predominant features were formation of transverse cracks and brittle fracture. Delamination of the fragments, characteristic for fracture (cracking) mechanism, from coating B can be attributed to the high presence of oxides comparing to the coating A (Figs. 3b and 3c).

Mean values of the coefficient of friction from CLST mode, for all tested materials are shown in Table 3. They increase with increase of normal load, but shows tendency for stabilization.

Table 3. Mean values of the coefficient of friction

Normal load, N	Material		
	A	B	SL 26
20	0.05	0.05	0.08
40	0.07	0.08	0.11
60	0.11	0.09	0.22
80	0.16	0.11	0.28
100	0.19	0.12	0.29

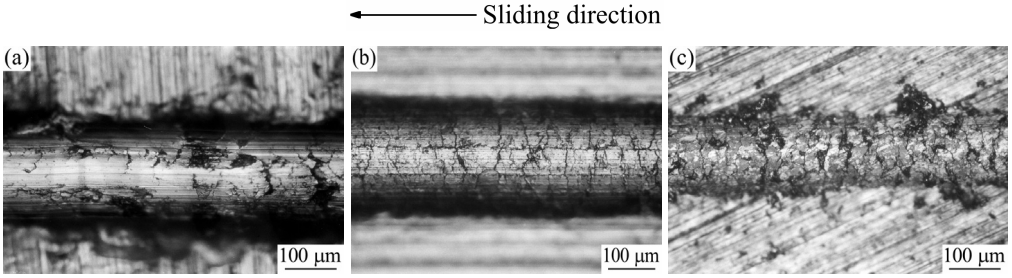

Figure 3. Wear scar appearance (OM) under the normal load of 60 N: a) SL 26, b) Coating A and c) Coating B

Wear volumes were calculated from wear scars profiles. Some of the scars profiles are shown in Figure 4.

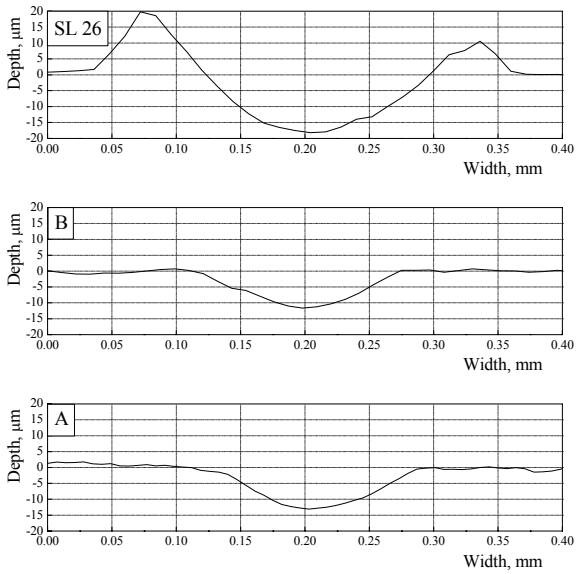

Figure 4. Wear scars profiles for normal load of 60 N

Wear rate of the tested materials increase with increase of normal load, but not linearly (Fig. 5).

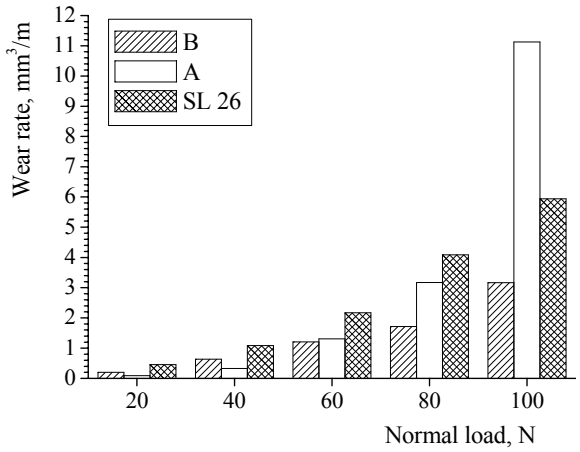

Figure 5. Wear rates of tested materials for different normal loads

There was no direct correlation between wear rates and hardness of tested materials. Gray cast iron as the softest material proved as the worse, while both coatings appeared as a satisfactory solution from the aspect of abrasive wear resistance.

4. CONCLUSION

Scratch test offers relatively easy and quick comparison of different materials on abrasive wear, with good reproducibility of the results, and it is suitable method for evaluation of thick coatings abrasive wear resistance.

Coefficient of friction and wear resistance of tested materials showed dependence on their hardness as well as the type of wear mechanism.

From engineering point of view, for lower loads, both coatings showed satisfactory values of friction coefficient and abrasive wear resistance in comparison with gray cast iron.

Between two coatings, coating B showed better overall tribological properties.

LITERATURE

[1] Khruschov, M.M., *Resistance of metals to wear by abrasion, as related to hardness*, International Conference on Lubrication and Wear, London (UK), 1-3.10.1957, Proceedings, pp. 654-658

[2] Khruschov, M.M., *Principles of abrasive wear,* Wear, 28, 1974, pp. 69-88

[3] Gold, P.W., *Tribology Script 2003*, Institute for Machine Elements and Machine Design, RWTH-Aaechen, Script, 2003, p. 58, Online, Internet at: http://www.ime.rwth-aachen.de/Lehre/Triboumdruck_E/index.html

[4] *Abrasive Wear Resistance*, Industrial Lubrication and Tribology, 43, 3, 1991, pp. 14-26

[5] *Aluminium in Automotive Industry*, European Aluminium Association, Brochure, p. 8, Online, Internet at: http://www.eaa.net/downloads/auto.pdf

[6] Williams, J.A., *Analytical models of scratch hardness*, Tribology International, 29, 8, 1996, pp. 675-694

[7] Vencl, A., Mrdak, M., Cvijović, I., Microstructures and tribological properties of ferrous coatings deposited by APS (Atmospheric Plasma Spraying) on Al-alloy substrate, FME Transactions, 34, 3, 2006, pp. 151-157

[8] *Turbojet engine - standard practices manual*, Part No 582005, Pratt & Whitney

[9] EN 1071-3:2002, *Advanced technical ceramics - Methods of test for ceramic coatings - Part 3: Determination of adhesive and other mechanical failure modes by a scratch test*